

Estimation of Effects of Underwater Acoustic Channel Capacity Due to the Bubbles in the High Frequency Near the Coastal Area

Guoqing Zhou*, Taebo Shim*, Young-Gyu Kim**

*Underwater Acoustic Communication Institute, Soongsil University, Korea

**Agency for Defense Development, Korea

(Received May 16, 2008; revised June 30, 2008; accepted July 23, 2008)

Abstract

Measurements of bubble size and distribution in the surface layer of the sea, wind speed, and variation of ocean environments were made continually over a four-day period in an experiment conducted in the South Sea of Korea during 17-20 September 2007. Theoretical background of bubble population model indicates that bubble population is a function of the depth, range and wind speed and bubble effects on sound speed shows that sound speed varies with frequency. Observational evidence exhibited that the middle size bubble population fit the model very well, however, smaller ones can not follow the model probably due to their short lifetime. Meanwhile, there is also a hysteresis effect of void fraction. Observational evidence also indicates that strong changes in sound speed are produced by the presence of swarms of micro bubbles especially from 7 kHz to 50 kHz, and calculation results are consistent with the measured data in the high frequency band, but inconsistent in the low frequency band. Based on the measurements of the sound speed and high frequency transmission configuration in the bubble layer, we present an estimation of underwater acoustic channel capacity in the bubble layer.

Keywords: *Bubble Size and Distribution, Bubble Effect, Sound Speed and Void Fraction, Clustered Bubble Clouds, Wind-driven Sea Surface, Underwater Acoustic Channel Capacity*

1. Introduction

As far as we know, gas bubbles in the ocean are the most efficient sound scatters. This is due to the fact that in a wide frequency range this scattering is of a resonant nature [1]. The resonant scattering cross section of an air bubble near the ocean surface is approximately 1000 times its geometrical cross section. The resonant bubbles not only scatter but also absorb the acoustic energy, as well. Furthermore, at sufficiently high concentrations they markedly

change the compressibility of water and then the sound speed and attenuation coefficient.

It has also been known that a layer of micro bubbles is formed under the ocean surface due to the winds exceeding a threshold of a few meters per second [2]. As the acousticians recognized it, they began to study the physical nature of the bubble layer. Hall [3] presented a comprehensive model of bubble spectrum for a range independent layer which depends on bubble radius, depth, and wind speed. Another comprehensive model describing the various stages of development of the bubble plume is developed by Monahan [4], [5]. Carey and Fitzgerald [6] adopted the estimation of void fraction and lifetimes from

Corresponding author: Taebo Shim (tbshin@ssu.ac.kr)
Dept. of Electric Engineering, Soongsil Univ., Sangdo 5-dong,
Dong jak-gu, Seoul, 156-743

Monahan's model to research the problem of sound emission by bubble clouds. They found that the bubbles acted as compact monopole sources of ambient noise at frequencies below 500 Hz. Jorge C. etc. [7], use a simple model to parameterize different stages of the assemblages of micro bubbles in a wind-driven sea surface [15]. Buckingham [13], [14] focused on the acoustic transmission in ocean-surface waveguides and Dahl [16], [17] discussed the contribution of the bubbles to the high frequency sea surface backscatter.

In this paper, firstly, we analyze the dataset obtained from the sea experiment conducted in the south sea of Korea during 17-20 September 2007. Secondly, we compare the bubble population model and void fraction model with the observed data. At last, high frequency transmission channel capacity in the bubble layer is estimated.

The outline of this paper is as follows. Section 2 provides theoretical background of bubble population and bubble effect on sound speed. In section 3, the measurements are presented. In section 4 measurement of the bubble size and distribution and the effects on sound speed are provided. In section 5, estimation of transmission channel capacity in the bubble layer is discussed. A summary is given in Section 6.

II. Theoretical Background of Bubble Population and Its Effect on Sound Speed

In underwater acoustics, the compact patches of bubbles are usually referred to as clouds or plumes without distinction. Monahan [5] assumed the existence of three types of (α, β, γ) plumes and associated two of them with stages of whitecaps: stage A, which is associated with the crest of the spilling breaker, and stage B, which is associated with the foam patch. The α -plume is the subsurface extension of the stage A whitecap. Although they present the highest void fraction $O(10^{-1} - 10^{-2})$, they are very small in size and have a very short lifetime (< 1 s). The α -plume quickly decays into β -plume once the momentum of

the downward moving jet associated with the breaking wave is dissipated. Accordingly, the stage A whitecap evolves into a foam patch (stage B whitecap). The β -plumes present a much smaller void fraction $O(10^{-3} - 10^{-4})$ and are attached to the foam patch. That is, the stage B whitecap is the top of the β -plume. They are spatially much bigger than the α -plume and have longer lifetimes (about 4 s). The β -plume then evolves into a γ -plume and eventually detaches from the originating whitecap. The γ -plumes have an even lower void fraction, much larger dimensions, and longer lifetimes (10-100 times longer) than the β -plume. The γ -plume decays into a weak stratified background layer.

The bubble population for each of the different assemblages of bubbles will be assumed to be represented by the genetic functional form [5]

$$n(a, z, u) = N_0 G(a, z) Z(z) U(u) \quad (1)$$

where N_0 is a constant, a is the bubble radius, z is the depth, and u is the wind speed 10 m above the sea surface. G is the functional form for the spectral shape, Z is the depth dependent function and U is the wind speed function.

For the functional form from spectral shape G which can be described as

$$G(a, z) = \begin{cases} \left[\frac{a_{ref}(z)}{a} \right]^4, & a_{min} \leq a \leq a_{ref}(z) \\ \left[\frac{a_{ref}(z)}{a} \right]^{x(z)}, & a_{ref}(z) \leq a \leq a_{max} \end{cases} \quad (2)$$

$$a_{ref}(z) = 54.4 \mu m + 1.984 \times 10^{-6} z$$

$$a_{min} = 10 \mu m, a_{max} = 1000 \mu m$$

and
$$x(z) = 4.37 + \left(\frac{z}{2.55} \right)^2$$

The depth dependent function which can be described as

$$Z(z) = \exp \left[-\frac{z}{L(u)} \right] \quad (3)$$

$$\text{where } L(u) = \begin{cases} 0.4m, u \leq 7.5 \text{ m/s} \\ 0.4 + 0.115(u - 7.5), u > 7.5 \text{ m/s} \end{cases}$$

The wind speed function U can be approximated as

$$U(u) = \left(\frac{u}{13}\right)^3 \quad (4)$$

The air void fraction ν can be written [8]

$$\nu(z) = \frac{\nu(0)}{J(0)} e^{-\nu(0) J(z)} \quad (5)$$

where

$$J(z) = \int_{z_{\min}}^{z_{\max}} \nu(z) G(a, z) dz$$

$$= \frac{4}{3} \pi a_{\text{ref}}^4(z) \left\{ \ln \frac{a_{\text{ref}}(z)}{a_{\min}} + \frac{1 - \left[\frac{a_{\text{ref}}(z)}{a_{\max}} \right]^{x(z)-4}}{x(z)-4} \right\}$$

$$\text{and } \nu(0) = V_{10} \left(\frac{u}{10}\right)^3, \quad V_{10} = 9.29 \times 10^{-7}$$

$$J(0) = 1.275 \times 10^{-16} \text{ m}^4$$

The presence of oscillating bubbles causes the medium to be dispersive. When the sound frequency is above the resonant frequency of minimum bubbles, the corresponding sound speed is given as [8]

$$c_m^{-2} = c_0^{-2} - \int_{a_{\min}}^{a_{\max}} \frac{4\pi n a}{(2\pi f)^2} da \quad (6)$$

where C_m is the sound speed of water with the bubble mixture and C_0 is the sound speed of the water in the absence of bubbles.

In the following section, we will compare the bubble population model and bubble effect on sound speed with the experiment data.

III. South Sea Measurements

3.1. Preliminary of Experiment

A four-day experiment of measuring the bubble size and distribution, wind speed, and variation of ocean environment was conducted in the South Sea of Korea (34-48-00 N, 128-49-50 E) during 17-20 September 2007.

Fig. 1 shows the experimental apparatus and layout for measuring the bubble effects on high frequency transmission. The measuring equipments are ABS, XSV, SBE25, SBE39, Tx MOBY, Rx VLA, Rx HLA, and ADCP aligned from left to right. The ABS (acoustic bubble spectrometer) is a device that measures bubble size distribution and void fraction

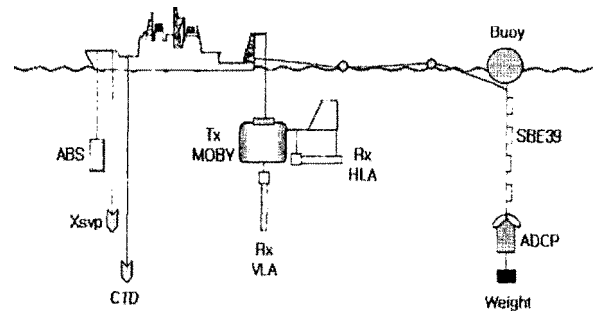


Fig. 1. Experimental apparatus and layout for measuring bubble effect on high-frequency transmission.

Table 1. Experimental apparatus configurations.

Category	MOBY	Rx Array	ADCP	ABS	XSV	SBE25	SBE39
Measure Subject	Pulse Transmission	Pulse Receive	Advection Currents	Bubble Distribution	Sound Speed	CTD	TD
Mount Methods	Deeping	Deeping	Mooring	Deeping	Deeping	Deeping	Mooring
Mount Height (m)	5	5	20	1,3,5	-	-	1~20
Measure Period	10~15 Second	1/50K	2 Second	1 Hour	1 Hour	1 Hour	10 Second
Frequency (kHz)	5~8	5~8	1200	500	-	-	-

of bubbles in liquids. The SBE39 is a high-accuracy temperature recorder and the SBE25 measures conductivity, temperature and pressure in the sea. The ADCP (Acoustic Doppler Current Profiles) provides the advection currents and the XSV measures the sound velocity in the test ocean domain. The Tx MOBY, Rx VLA and Rx HLA are used to pulse transmission and reception, of which results show the bubble effects on the high frequency transmission. Table 1 summarizes the instrumentation for this field study.

3.2. Variation of the ocean environment

The ADCP use the Doppler effect by transmitting sound at a fixed frequency and listening to echoes returning from sound scatters in the water [10], [12].

Fig. 2 shows the measurement of pitch, roll, and heading using ADCP. The measurement of advection currents varied with depth shown in Fig. 3 From the observation, we can clearly see that advection currents in the ocean surface layer are very low.

The wind speed measurements were made with a Coastal Climate anemometer mounted above the sea surface on the stern of the research vessel. Fig. 4 shows the measurements of the wind speeds from 18 to 19 September 2007. The observed results show that the wind speeds in the two days changed very much even though at one hour interval, so it is beneficial for us to focus on the degree how the bubble distribution depends on the wind speed.

IV. Measurement of the Bubble Size and Distribution and the Effects on Sound Speed and Attenuation

The ABS (acoustic bubble spectrometer) is an acoustics device that measures bubble size distribution and void fraction of bubbles in liquids [9]. The measurement is based on a dispersion relation for propagation of sound waves through a bubbly liquid [11].

Fig. 5 shows the comparison of bubble population

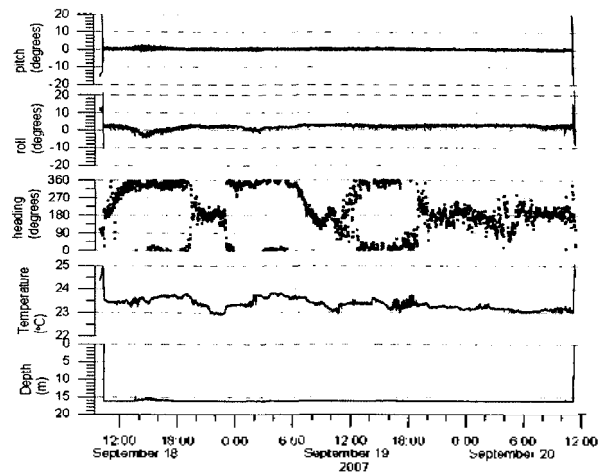


Fig. 2. The measurement of pitch, roll and heading from 18 September to 20 September 2007.

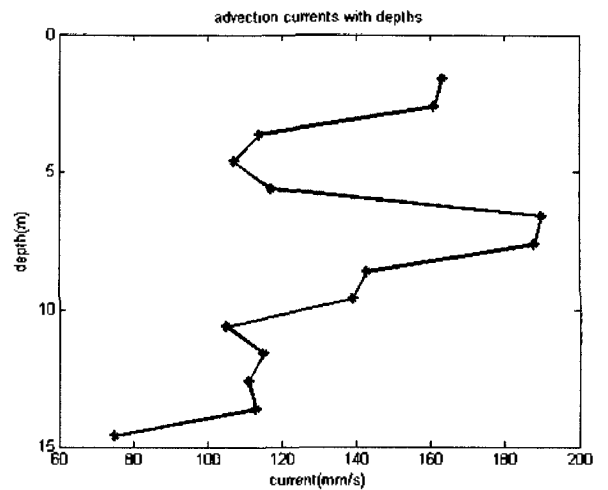


Fig. 3. The measurement of advection currents at ten o'clock 19 September 2007.

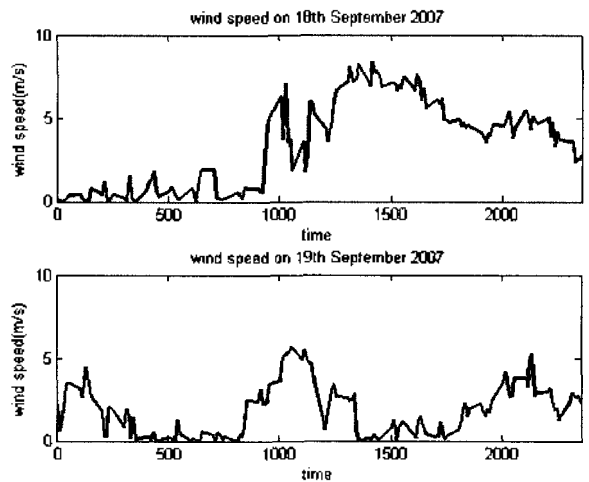


Fig. 4. The measurement of wind speed from 18 September to 19 September 2007.

estimated from the Hall's model and observed from

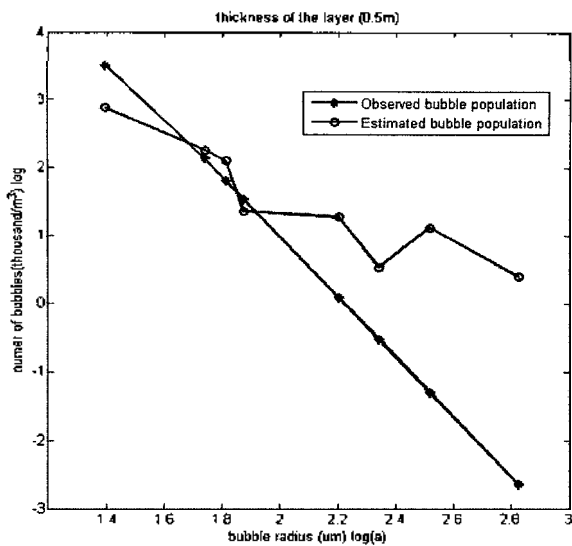


Fig. 5. Comparison of bubble population at the thickness of 0.5 m layer.

the experiment. The results indicate that the observed bubble population follows the Hall's model very well when the bubble radiuses are in the middle size from 44 μm to 85 μm . However, the small size bubbles are not fit with the model. This is probably due to the very short life time.

Fig. 6(a) shows the measured wind speed. In Fig. 6(b), the dotted line shows the void fraction which calculated from equation 5, with the modified constant value of $J(0) = 0.8 \times 10^{-14}$. Meanwhile, the starred line shows the observed void fraction value during the same period with wind speed measurements. The results indicate that void fraction of theoretical value varied immediatly following the wind speed pattern. However, observed value of the void fraction has the hysteresis appcarance, probably due to the time delay to form the bubble by the wind. But it is difficult to ascertain the delay time to lack of enough data.

Fig. 7 shows the measurement of the sound speed ratio at 0.5 m depth at the simultaneous time as the measurement of the bubble size and distribution. From the data, the results show that the presence of bubbles leads to a significant variation in the phase speed, with strong dispersion over the frequency range from 7 kHz to 50 kHz.

Fig. 8 indicates the comparison of the sound speed ratio calculated from the sound speed model with the

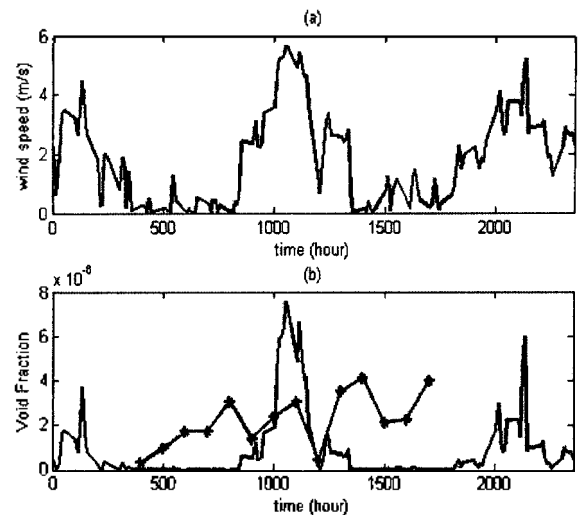


Fig. 6. Comparison of void fraction at the thickness of 0.5 m layer.

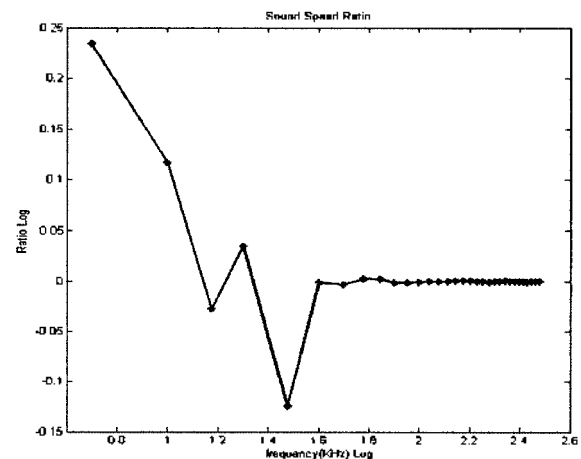


Fig. 7. The measurement of sound speed ratio at ten o'clock 19 September 2007 of 0.5 m depth.

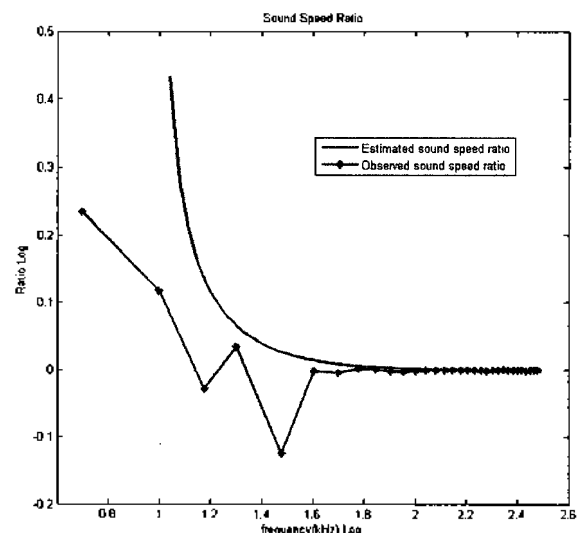


Fig. 8. The comparison of sound speed ratio from the sound speed model with the measurement values at ten o'clock 19 September 2007 of 0.5 m depth.

measured values due to bubble effect. From which calculation results are consistent with measured data in the high frequency band but inconsistent in the low frequency band. That may be realized from the formula of the sound speed model directly. The calculated data has finite value when $\frac{1}{c_0^2} > \int_{a_{min}}^{a_{max}} \frac{4\pi na}{(2\pi f)^2} da$, but according to equation (6) when $\frac{1}{c_0^2} < \int_{a_{min}}^{a_{max}} \frac{4\pi na}{(2\pi f)^2} da$, it has no value.

In the following section, we will estimate the channel capacity in the bubble layer using the measured sound speed and Ray theory.

V. Estimation of Channel Capacity in the Bubble Layer

The effects of micro-bubbles may be particularly significant for the performance of high frequency sonar operating in the range of tens to hundreds kHz.

Fig. 9 shows the source and receiver array for the pulse transmission experiment in the bubble layer. A vertical array was suspended at a depth of about 5.6 m off the stern of the ship. The array was held in position to prevent uncontrolled rotation and heave motion and the array's pitch angle θ_p was remotely monitored and set. For these measurements the transducer was pitched upward with approximately 1.8 degree (measured remotely with tilt meter), and pulse length was 40 ms, which set angular resolution to approximately 0.1 degree, and the frequency was set to 30 kHz.

First, we calculate the sound speed versus depth profile using data from the SBE25 CTD. The ex-

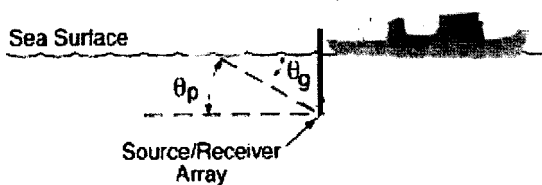


Fig. 9. The source and receiver array layout for pulse transmission.

ponential sound speed profile follows the formula:

$$c_b(z) = c(z) + \Delta c e^{-z/l} \quad (7)$$

Where z is the depth from the surface, Δc is the surface sound speed anomaly, l is the e-folding depth, $c(z)$ is the bubble free sound speed and $c_b(z)$ is the sound speed in the bubbly medium.

Measured Δc is 9 m/s and based on the bubble population, the L is equal to 2.1 m. The comparison of sound speed from exponential model with the observational value from CTD is shown in Fig. 10. The diagram indicates that the sound speed profile in the bubble layer can be approximated by an exponential model.

In order to estimate the underwater acoustic channel capacity, the channel configurations are shown in Table 2.

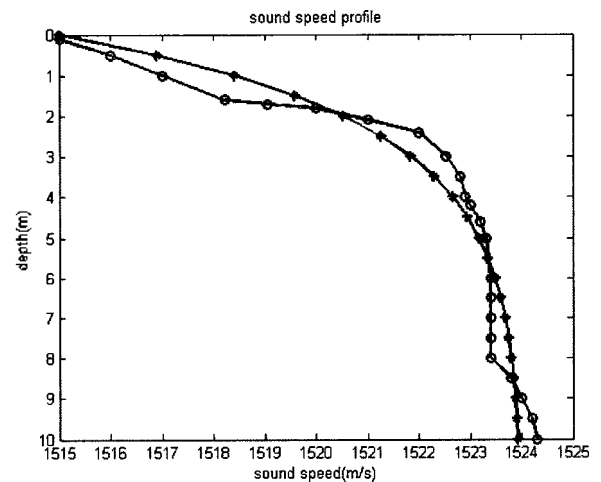


Fig. 10. The sound speed profile and the model of the sound speed profile; the star line denote the exponential model of the sound speed profile and the dot line is the measurement of the sound speed.

Table 2. Channel Configuration.

Channel depth	45 m
Source depth	5.6 m
Receiver depth	6 m
Range	1500 m
Bottom material	Muddy sand
Wind speed	6 m/s
Signal carrier frequency	30 kHz
Bandwidth	10 kHz

The ray diagram in Fig. 11 shows rays emanating from the source of depth 5.6 m based on the former sound speed. Here, the sound field close to the sea surface begins to diverge with decreasing launch angle owing to refraction. With still smaller launch angle, rays undergo downward refraction, eventually producing a shadow zone and caustic region.

The transmission loss (TL) can also be calculated from the Bellhop ray software [18], [19]. Fig. 12 shows the TL varied with range for the experiment. We can clearly see that TL and phase shift is severely affected by the existence of bubbles, and these effects will therefore affect the performance of sonar in the high frequency transmission.

Based on the theoretical derivation of UACH capacity [20], [21] and sound transmission experiment results from this experiment, estimation of underwater acoustic channel capacity in the bubble layer is shown in Fig. 13. The source power is assumed 193 dB//uPa²/Hz and the source center frequency is assumed at 30 kHz with bandwidth 5 kHz. From Figure 14, we can see that the estimated channel capacity decreases with the range, which is presumably due to the path loss of acoustic energy in the ocean. We also find that the channel capacity nonlinear varied with the range which maybe due to the random transmission loss.

VI. Conclusion

Due to the disparity of data available on subsurface bubble layer and the many intervening parameters, to infer a precise bubble population and the effects of bubbles on high frequency transmission is too complex. In this paper, we only analyze the dataset obtained from the sea experiment conducted in the south sea of Korea. Experimental results indicate that strong changes in sound speed and attenuation are produced by the presence of swarms of micro bubbles. Measured results also indicate that bubble layer beneath the sea surface may show an exponential sound speed profile. Based on measurements of the

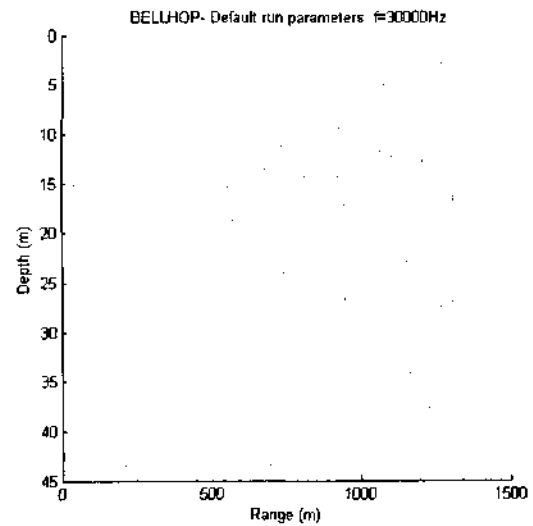


Fig. 11. The ray diagram for the experiment conducted on 19 September 2007.

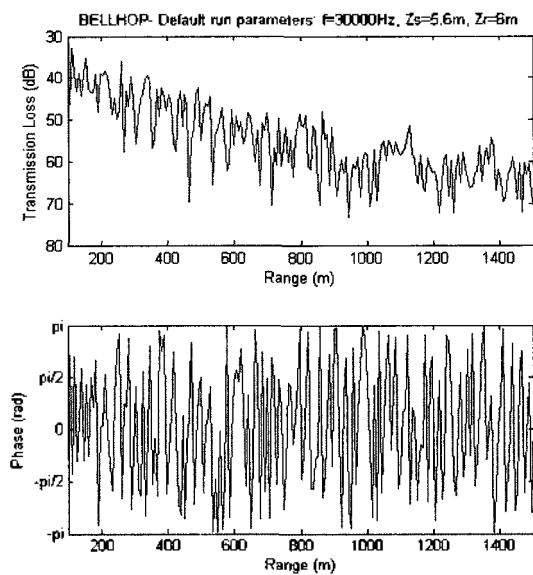


Fig. 12. The transmission loss and phase shift for the experiment conducted on 19 September 2007.

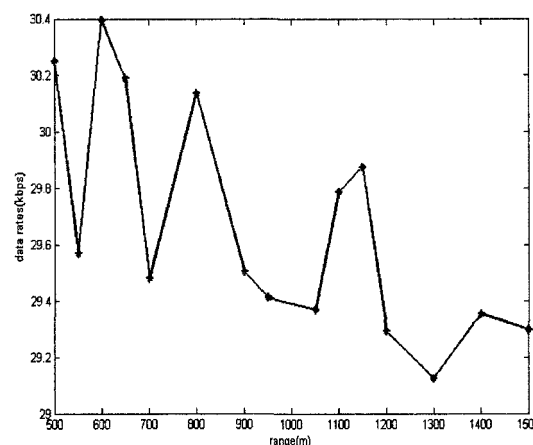


Fig. 13. Channel Capacity in the bubble layer.

sound speed and the transmission, the underwater acoustic channel capacity was estimated in the bubble layer using the derived model [22].

References

1. L.M. Brekhovskikh and Y.P.Lysanov *Fundamentals of Ocean Acoustics* (2001), pp.250–273.
2. S.A. Thrope, "On the clouds of bubbles formed by breaking waves in deep water and their role in the air sea gas transfer" *Philos. Trans.R. Soc. London Ser.*, 155–210, 1982.
3. M. V. Hall, "A comprehensive model of wind-generated bubbles in the ocean and predictions of the effects on sound propagation at frequencies up to 40 kHz," *J. Acoust. Soc. Amer.*, **86**, 1103–1116, 1989.
4. E. C. Monahan, "Whitecap coverage as a fully monitorable indication of the rate of bubble injection into the oceanic mixed layer," in *Sea Surface Sound*, edit by B. R. Kerman (New York: Academic, 1998), pp.85–96.
5. E. C. Monahan and M. Lu, "Acoustically relevant bubble assemblages and their dependence on meteorological parameters," *IEEE J. Oceanic Eng.*, **15**, 340–349, 1990.
6. W. M. Carey and J. W. Fitzgerald, "Low frequency noise from breaking waves," *J. In Kerman op. cit.*, 277–304, 1993.
7. J. C. Novarini, R. S. Keiffer, and G. V. Norton, "A model for variations in the range and depth dependence of the sound speed and attenuation induced by bubble clouds under wind-driven sea surfaces" *IEEE J. Oceanic Eng.*, **23**(4), 423–438, 1998.
8. J. S. Zhang, *Sound speed in bubble film of ship wakes* (Science in China Series G : Physics, Mechanics & Astronomy 2008), pp. 64–71.
9. M. A. Ainslie "Effect of wind-generated bubbles on fixed range acoustic attenuation in shallow water at 1–4 kHz" *J.Acoust.Soc. Am.*, 3513–3523, 2005.
10. R. Duraiswami, S. Prabhukumar and G. L.Chahine "bubble counting using an inverse acoustic scattering method" *J.Acoust.Soc.Am.*, 2699–2717, 1998.
11. R. E. Callisch, M. J. Miksis, G. C. Papanicolau, and L. Ting, "Effective Equations for wave propagation in bubbly liquids," *J. Fluid Mech.* **153**, 259–273, 1985.
12. *Acoustic Doppler Current Profiler, Principles of Operation for a Practical Primer* (1996).
13. M. J. Buckingham "Sound Speed and Void Fraction Profiles in the Sea Surface Bubble Layer" *Applied Acoustics*, 225–250, 1990.
14. M. J. Buckingham "On Acoustic Transmission in Ocean- surface Waveguides" *Philosophical Transactions: Physical Science and Engineering*, 513–555, 1991.
15. J. C. Novarini, R. S. Kriffer, and G. V.Norton "A model for variations in the range and depth dependence of the sound speed and attenuation induced by bubble clouds under wind-driven sea surfaces" *IEEE Journal of Ocean Engineering*, 423–437, 1998.
16. T. C. Weber, A. P.Lyons, and D. L.Bradley "acoustic propagation through clustered bubble clouds" *IEEE Journal of Ocean Engineering.*, 513–523, 2007.
17. P. H.Dahl, " The contribution of the bubbles to high frequency sea surface backscatter" *J.Acoust.Soc.Am.*, 769–780, 2002.
18. S. Richards and T. Leighton "High frequency sonar performance for littoral operations—the effects of suspended sediments and micro-bubbles" *Journal of Defense Science.*, 1–7.
19. M. B. Porter, *The KRAKEN Normal Mode Program and Bellhop Ray Program* (SACLANT Undersea Research Center).
20. G. Zhou, J. S. Cho, and T. B. Shim, "Underwater Acoustic Communication Channel Capacity in the Sloping Condition", KASI-ASK Joint Conference on Acoustic, 135–138, 2007.
21. G. Zhou and T. B. Shim, "Adaptive Transmission Technique in Underwater Acoustic Wireless Communication", LNCS ICES2007., 268–277, 2007.
22. G. Zhou and T. B. Shim, "Simulation Analysis of High Speed Underwater Acoustic Communication Based on a Statistical Channel Model", IEEE CISP 2008, 2008.

[Profile]

• Guoqing Zhou



2002.7: B.S. in Automation; Dept. of information and electronic, Shandong University of Science and Technology (SDUST), China
 2002.7–2006.7 Research Engineer: Science and Technology Company of SDUST, China
 2006.9–Present: M.S. degree of underwater communication, Dept. of Electronic Engineering, Soongsil University, Korea
 Interested area: Underwater Acoustic Communication, Underwater Acoustic Signal Processing

• Taebo Shim



1974: B.S. in Physics Oceanography, Seoul National University, Korea
 1980: M.S. in Physics Oceanography, Seoul National University, Korea
 1986: Ph.D. in Physics Oceanography, Louisiana State University, USA
 1986–2005: Principle Researcher: Agency for Defense Development (ADD), Korea
 2005–Present: Professor: Department of Electric Engineering, Soongsil University, Korea
 Interested area: Underwater Acoustic Communication, Underwater Acoustic Signal Processing, Underwater Acoustic Image Processing

• Young-Gyu Kim

The Journal of the Acoustical Society of Korea, Vol.25, No.7, 2006.